PAPER

Check for updates

De Novo designed 13 mer hairpin-peptide arrests insulin and inhibits its aggregation: role of OH−π interactions between water and hydrophobic amino acids†

Meghomukta Mukherjee, Nilanjan Banerjee and Subhrangsu Chatterjee [ID] *

Background: Protein aggregation in the cellular systems can be highly fatal causing a series of diseases including neurodegenerative diseases like ALS, Alzheimer, Prion Diseases, Parkinson's and other diseases like type II diabetes. To date, there is no crucial mechanism invented that shows how a protein molecule unfolds or misfolds. Insulin fibrillation in type II diabetes is an alarming event that brings every year deaths of millions of people around the globe. Pharmaceutical companies are still in the cultivation of finding newer therapeutic agents which halt/impede insulin aggregation to combat diabetes II and improve the patient's life expectancy. *Methods and Results*: Here in this report, we have engineered four short 13 mer peptides (N-term-DMYY-RYNGKVWWR, N-term-DITT-RYNGKVWWR, N-term-DIFF-RYNGKVWWR, N-term-KVYY-RYNGKVWWR) which target monomeric insulin in its globular form. The *de Novo* designed peptides are found to be non-cytotoxic in human HEK293 cells. Among these four peptides, only DITT-RYNGKVWWR showed complete inhibition of insulin fibrillation, whereas DIFF-RYNGKVWWR and DIYY-RYNGKVWWR and KVYY-RYNGKVWWR lost their functionality to impede insulin aggregation to a great extent. High-resolution multi-dimensional NMR experiments portrayed the 13 mer sequences of peptides in the beta-hairpin forms. A series of biophysical techniques like CD, ThT assay, DLS, SEM, ITC, size-exclusion chromatography, and molecular dynamics simulation strongly evidenced inhibition of insulin fibrillation by N-term-DITT-RYNGKVWWR, compared to those by the other peptides. *Conclusion and significance*: Here we tried to unravel how DITT-RYNGKVWWR could impede insulin fibrillation.

1. Introduction

Protein aggregations have been found to be associated with many human diseases such as Alzheimer's disease, Creutzfeld-Jacob, type-2 diabetes, Parkinson's, *etc.*[1,2] The protein aggregates to form amyloid plaques under several environmental conditions.[3,4] This amyloid fibril formation undergoes several stages-including aggregation of soluble oligomers, the formation of protofibrillar structure and their assembly to mature fibrils.[5,6]

Insulin is a globular protein hormone that has several functions including regulation of lipid synthesis, regulation of enzymatic activity but the majorly it regulates glucose metabolism in cells.[7,8] Insulin has the propensity to undergo aggregation in its partially unfolded state.[9–11] The previous report states that in Parkinson's disease affected type II diabetic patients;

insulin starts to aggregate and deposits into the cells.[12] *In vitro* studies proposed by Walsh G. *et al.* states that insulin aggregation disables the normal insulin function *i.e.* regulating the cellular glucose level and thus concealing the therapy for type 2 diabetes.[13] In fact, regular intravenous injection of insulin results in its deposition into the dermal site of injection. This condition is known as 'amyloidoma'.[14] In such a condition, insulin becomes futile for treating diabetes.[15]

It is known that heat treatment of insulin, (especially in acids), results in the formation of insulin fibrils.[16] This process of fibril formation involves nucleation, growth, and precipitation and is dependent on pH (in the acid range) and the type of acid in which fibrils are formed. Insulin fibrils are long and unbranched with a marked degree of variations in the cross section.[17,18] Few reports propose the specific interactions (between the amino acid residues) that lead to insulin fibrillation which induce insulin dimerization.[9,24,25] There have been many reports on the prevention of fibrillation of insulin by organic and inorganic molecules,[20–23] however, little is known about the underlying molecular mechanisms of inhibition of insulin fibril formation. Identification of the interacting

Department of Biophysics, Bose Institute, P 1/12 CIT, Scheme VII M, Kankurgachi, Kolkata 700054, India. E-mail: subhro_c@jcbose.ac.in

domains in the aggregates has been the subject of research for many years.[19]

Insulin unfolding is initiated from the C-terminal of B-chain. According to Hua *et al.* partial unfolding in B-chain increases the possibility of aggregation by exposing the non-polar side chains.[9] Residues responsible for such fibrillations are Phe1(B), Val2(B), Leu6(B), Phe24(B), and Tyr26(B). Eisenberg *et al.* suggested that the smallest fragment of B-chain 11-LVEALYL-17 (B) is responsible for the initiation of insulin aggregation. Brange *et al.* reports that desoctapeptide-(B23–B30) and despentapeptide-(B26–B30) are able to form fibrils.[19,26]

Designing peptide sequence which targets protein–protein interaction is a promising approach for drug designing. A study indicated that when β-strands are localized at the edge of β-sheets containing proteins they are found to prevent further fibril formation.[27,28] Based on this idea we designed these 13-mer β-hairpin peptides and hypothesized that these peptides might interact with protein that has a tendency to fibrillate in some environmental condition and impedes its fibrillation process. DITTRYNGKVWWR sequence was first idealized from 1,4 α-glucan branching enzyme. After choosing the sequence we made some selective modification to bring the perfect beta-hairpin structure. This sequence also fulfills the criteria to be a beta-hairpin peptide by maintaining the hydrophobic/hydrophilic ratio. We further modified the first four amino acid of the parent sequence and designed three more sequences that form the beta-hairpin structure. Since there was the previous report that states beta-hairpin peptides act as an inhibitor for amyloid formation,[29] it was our concern to find out the structural specificity of the beta-hairpin peptides which inhibits the fibrillation process. We kept the 9 residues RYNGKVWWR constant because the YNGK sequence helps in the formation of the beta-turn where VWWR formed beta-strand. Keeping this in mind cultivation of therapeutic agents targeting the C-terminal of B-chain of insulin would be of high interest to arrest insulin in its globular form and impede its aggregation to develop fibrils. The β-turn sequence was taken from the previous experiment.[29] The proteolytic degradation in the cellular system and membrane permeability limits the larger sized peptides to become a drug. So, in that case, small-sized peptides are desirable. To investigate the efficacy of four peptides against insulin a series of biophysical experiments have been performed. Isothermal Titration Calorimetry was ThT Assay was performed to check if the peptide can arrest the insulin fibril formation, CD spectroscopy was employed to check the secondary structural changes of insulin upon peptide binding, dynamic light scattering, nuclear magnetic resonance spectroscopy for peptide structure determination, saturation transfer difference NMR spectroscopy, SEM, size exclusion chromatography was executed. XTT assay was performed to evaluate the cytotoxicity of the peptides.

2. Methods and materials

2.1 Reagents

All the reagents for peptide synthesis were from Sigma and Merck. The bovine insulin is from Sigma.

2.2 Peptide synthesis

The four peptides were synthesized in solid-state peptide synthesizer from Aapptec endeavor 90. All the amino acids are F-moc linked. PyBOP was used as an activator of the reaction during peptide synthesis. We used DIPEA (*N,N*-diisopropylethylamine) as a base of the reaction. Also, the coupling reagent was DMF (*N,N*-dimethylformamide) and the de-coupling reagent was 20% piperidine. All the four peptides were synthesized and to provide stability to these peptides during synthesis it was acetylated at the end of the synthesis. The synthesized peptides were cleaved from the resin and side chain blockers by cleaving with trifluoroacetic acetic acid, anisol, phenol, tri-isopropanol saline. Then all the peptides were purified by reverse-phase HPLC. The purified peptides were further used to study insulin fibrillation.

2.3 ThT-assay

Thioflavin-T is a dye specific for the detection of fibrillation of proteins. It has an excitation wavelength at 440 nm while the emission wavelength at 480 nm. We prepared insulin in the citrate–phosphate buffer, pH 2.6. The concentration of insulin was 350 μM. All the four hairpin peptides were co-incubated with insulin monomers at the very beginning of the experiments. At several time intervals, the data were collected.

2.4 Circular dichroism

Secondary structural change of insulin over time was analyzed from circular dichroism. Insulin is a globular protein that shows a helical structure at 222 nm and 208 nm. All the spectra were analyzed by Jasco 815 circular dichroism spectropolarimeter at 25 °C. The final concentration of insulin was 350 μM. The scanning wavelength was from 200 nm to 260 nm. The speed of each scan is 100 nm s^{-1} and bandwidth 1 nm. The results of each spectrum were an average of 3 scans. Buffer's spectra were subtracted from the insulin spectra. All the spectra measured were time-dependent.
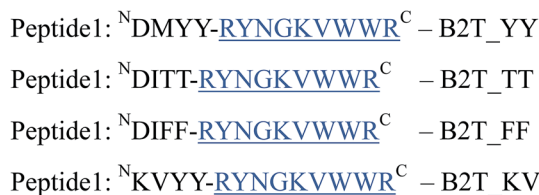
2.5 SEM (scanning electron microscopy)

Scanning electron microscopy is a low resolution instrument for taking images of a molecule's morphology. Insulin samples were prepared in 1 μM, 5 μM, and 10 μM concentration. Samples were coated with gold in Edward's S150 Sputter Coater before scanning. Finally, images were taken using the FEI QUANTA 200 scanning electron microscope. Insulin was mixed with the all four hairpin peptides in 1 : 1 ratio.

2.6 DLS (dynamic light scattering)

DLS studies were performed on Malvern nano dynamic light scattering equipment. The insulin sample was taken at a concentration of 350 μM in the presence and absence of hairpin peptides for analysis. All the samples were filtered through a microfilter containing a pore size of 0.2 μM.

The measured size was presented as the average value of 25 runs. Dynamics 7.10.0.10 software at optimized resolution was used for data analysis. The mean hydrodynamic radius (Rh) and

Peptide1: ^{N}DMYY-RYNGKVWWR^C – B2T_YY

Peptide1: ^{N}DITT-RYNGKVWWR^C – B2T_TT

Peptide1: ^{N}DIFF-RYNGKVWWR^C – B2T_FF

Peptide1: ^{N}KVYY-RYNGKVWWR^C – B2T_KV

Scheme 1 *De Novo* designed 13-mer peptides.

polydispersity (Pd) were estimated on basis of an autocorrelation analysis of scattered light intensity based on translational diffusion coefficient, by Stokes–Einstein equation: Rh ∼ KT = 6pgD250CW where Rh is the hydrodynamic radius, k is the Boltzman's constant, T is the absolute temperature, g is the viscosity of water and D25uC w is the translational diffusion coefficient.

2.7 Isothermal calorimetric titration

ITC experiment was carried out in 25 °C in VP ITC micro calorimeter equipment. The insulin solution was taken in the cell and hairpin peptides were taken in the syringe and the buffer was taken in the reference cell. We performed the experiment in citrate–phosphate buffer pH-2.6. The insulin solution was stirred at 300 rpm by the syringe. This titration of insulin with B2T peptides was performed of a total of 14 injections. The first injection was of 1 : l, which was not assumed in analysis, and remaining all the injections were of 3 μl. The heat of dilution was subtracted from the main titration data. After the equilibration was reached, then only the titration was started. All the data were analyzed in origin software. The heat change (ΔG) and the entropy change (ΔS) were calculated from the thermodynamics law equation. The buffer was subtracted from the results.

2.8 Size exclusion chromatography

Size exclusion chromatography was performed at room temperature in the Biorad torosh column. The insulin was taken in 1 mg ml^{-1}. Hairpin peptides were added in a 1 : 1 ratio. Three samples were separately run in the column. The total column volume was 50 ml. The void volume of the column was 15 ml. We start collecting the sample after the void volume was released. A total of 50 ml of the sample was collected from the column for each sample.

2.9 NMR (STD, TOCSY, and NOESY)

For performing STD NMR we prepared samples in 99.0% D$_2$O and the pH was adjusted as per requirement. NMR is a high-
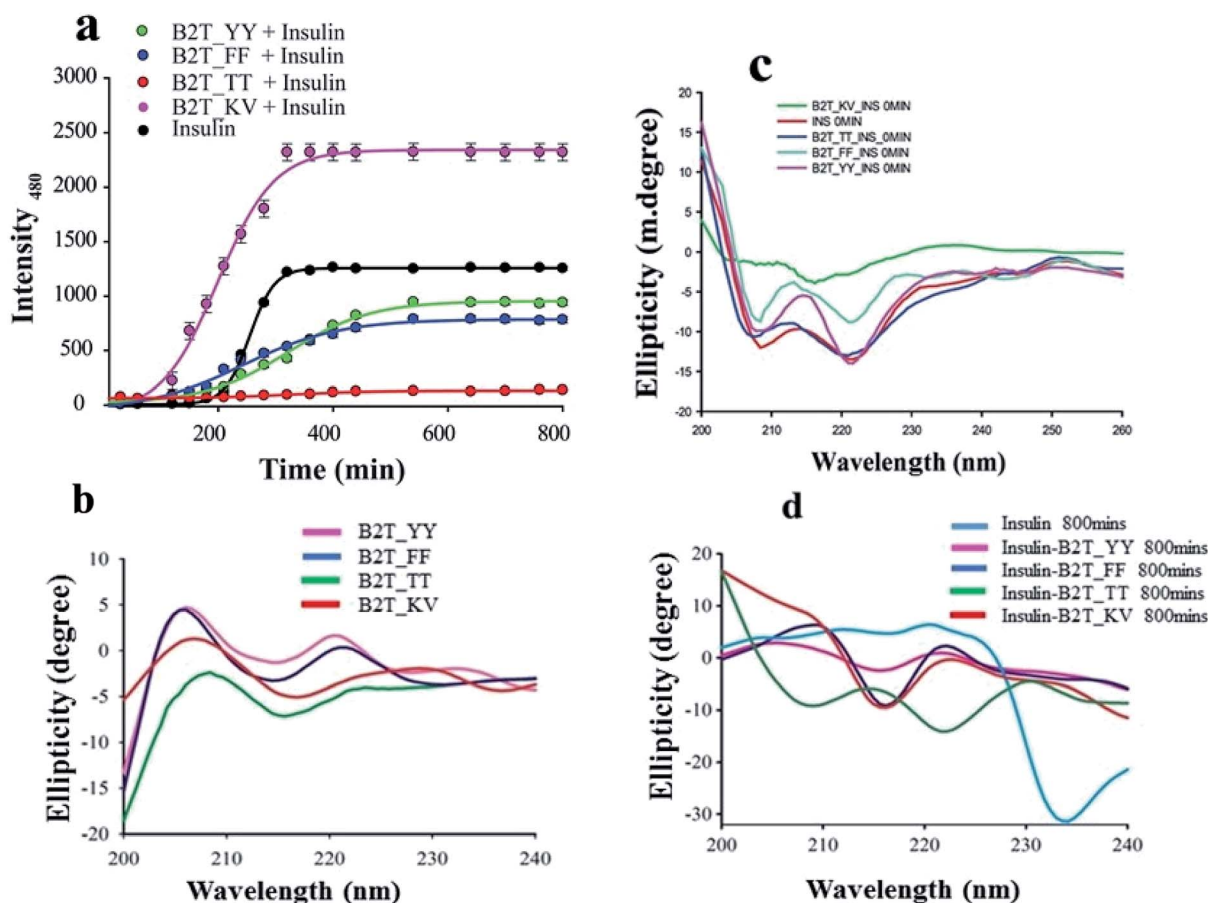

Fig. 1 (a) ThT-assay of insulin, insulin in presence of B2T_YY, B2T_TT, B2T_FF, and B2T_KV up to 800 min of incubation at 62 °C. (b) CD spectra of all peptides, (c) initial stage (0 min) of insulin and insulin presence of all four peptides and (d) CD spectra of insulin and all insulin peptide complex after 800 min of heat incubation.
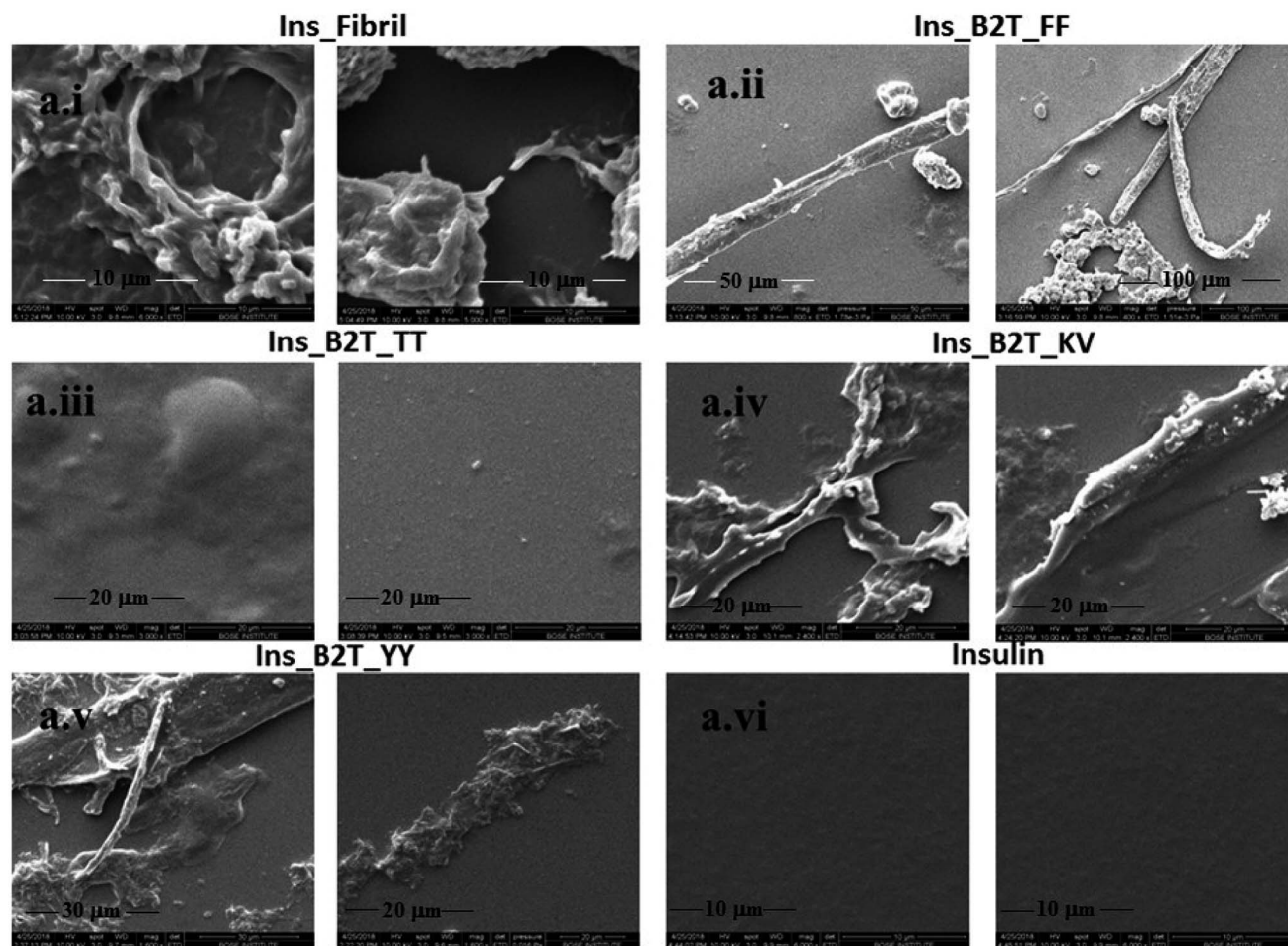
Fig. 2 SEM images of (a.i) Insulin after 800 min of heat incubation at 62 °C, (a.ii) insulin−B2T_FF complex after 800 min of heating, (a.iii) insulin−B2T_TT complex after 800 min of heating, (a.iv) insulin−B2T_KV complex after 800 min of heating, (a.v) insulin−B2T_YY complex after 800 min of heating, and (a.vi) insulin before heating at 62 °C.

resolution spectroscopy technique used to detect the structure, dynamics, and interactions between molecules. We carried out this NMR technique to check the molecular interaction between insulin and MB. All NMR spectra were recorded using a Bruker AVANCE III 500 MHz spectrometer equipped with a 5 mm SMART probe at 298 K. Data acquisition and processing were performed using Topspin 3.1 software. All NMR samples were prepared in 50 mM citrate–phosphate buffer, containing 10% D_2O and using TSP as an internal standard (0.0 ppm). Insulin powder was dissolved in 600 μl citrate–phosphate buffer (pH-2.6) with D_2O and TMS with it. STD NMR was done for three samples, reference, in the presence of insulin and in the absence of insulin. We performed the STD NMR experiment to find out the possible residues of the hairpin peptides interacting with the insulin monomer.

2.10 Docking

Docking was used by using online peptide docking software Z_DOCK.[30] 10 predicted docked models were given with REMD value by this server. The most common pose among the 10 models was chosen for a further simulation run.

2.11 Molecular dynamics simulation

Overall 5 systems were considered for simulation analysis *i.e.* all four peptides complexed with insulin and insulin in an unbound form. Simulations were performed with AMBER14. General Amber Force Field (GAFF)[31] which uses simple harmonic function and ff14SB forcefield[32] was used for parameterization of peptide–insulin complex. All systems were neutralized by adding counter-ions and further solvated with a 14 Å TIP3PBOX water model. The standard protocol of AMBER simulation was followed; two-step minimization, heating for 50 ps at 300 K, and equilibration phase for 1 ns. The macroscopic parameters like density, temperature, and RMSD of all the systems were equilibrated prior to production run. Equilibrated systems were used for further production run of 100 ns on an NPT ensemble at 300 K temperature and 1 atm pressure, with a step size of 2 fs.

2.12 Cell culture

HEK293 (gifted from Dr Samit Chattopadhay, Indian Institute of Chemical Biology) were maintained in complete DMEM (Himedia; AL007G) media, supplemented with 10% FBS (fetal
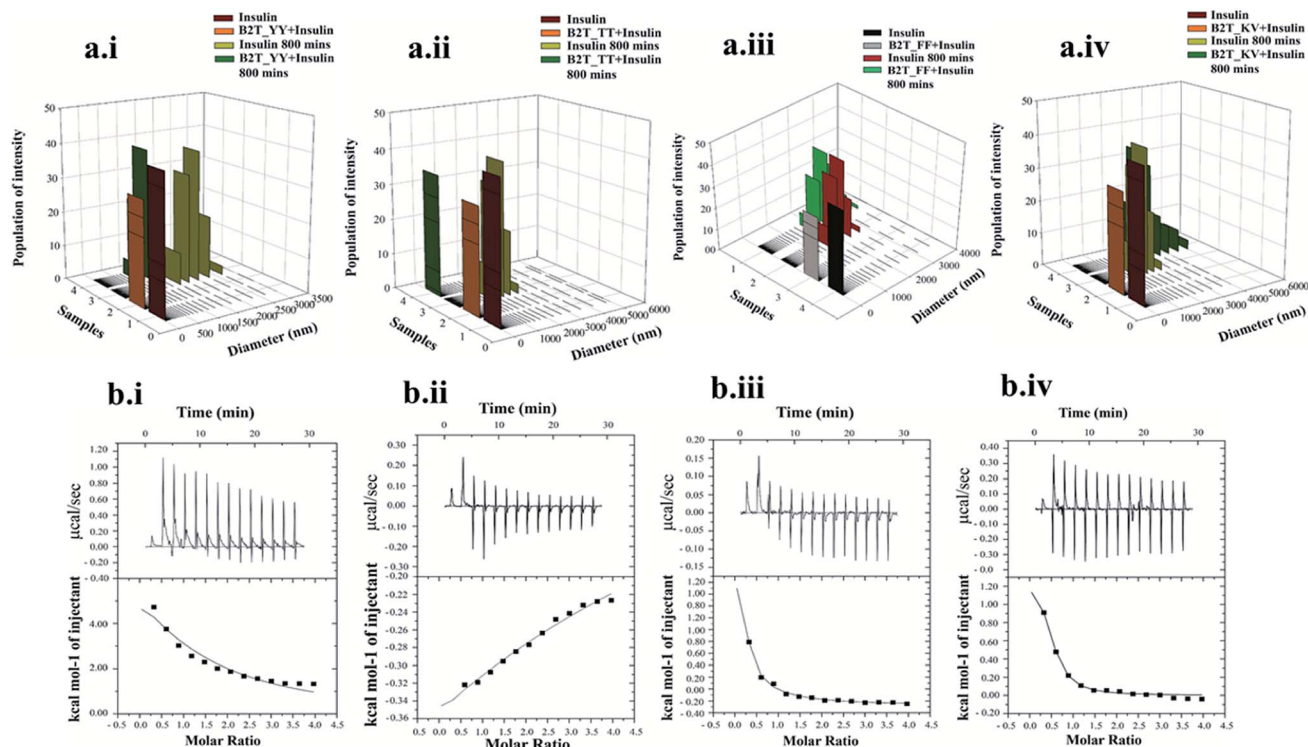
Fig. 3 DLS data of insulin and insulin−B2T_YY complex (a.i), insulin and insulin−B2T_TT complex (a.ii), insulin and insulin−B2T_FF complex (a.iii) and insulin and insulin−B2T_KV complex (a.iv) 0 min and 800 min of incubation. ICT data of insulin and B2T_YY, B2T_TT, B2T_FF and B2T_KV (b.i to b.iv respectively).

bovine serum), 1% penicillin and 1% streptomycin in a fully humidified incubator at 37 °C and 5% CO_2/95% air.

2.13 XTT assay

HEK293 cells were grown in DMEM medium supplemented with 10% FBS, 1% penicillin and 1% streptomycin. Cells were seeded into 96-well culture plates at a density of 1×10^4 cells per well and cultured overnight at 37 °C and 5% CO_2/95% air in a humidified incubator. The cells were then treated with varying concentrations of peptides (1 μM, 5 μM, 10 μM, 25 μM and 50 μM) in triplicate condition and incubated for 24 hours. The XTT dye (Cell Signalling) at a prescribed concentration was added after 24 hours and again incubated at 37 °C for 3 hours. The optical density of each well was then read at 450 nm using a BR Biochem Microplate Reader. The percent of cell viability of treated cells was calculated by the following equation:

$$(A_{\text{tested}} - A_{\text{media control}})/(A_{\text{drug-free control}} - A_{\text{media control}}) \times 100\%$$

where A is the mean value calculated by using the data from three replicate tests.

3. Results and discussion

The purpose of the current study is the inhibition of insulin fibrillation by *de novo* designed 13-mer peptides. The four 13-mer *de novo* designed peptides are N-DMYYRYNGKVWWR-C, N-DITTRYNGKVWWR-C, N-DIFFRYNGKVWWR-C, and N-

KVYYRYNGKVWWR-C which are denoted here in this study as B2T_YY, B2T_TT, B2T_FF, and B2T_KV respectively (Scheme 1).

3.1. Kinetics of insulin fibrillation and morphology analysis study by ThT-assay and SEM

ThT assay is one of the most effective and quantitative assays to evaluate amyloid fibril formation. From ThT-assay we observed that among the four hairpin peptides B2T_YY, B2T_FF, and B2T_KV showed an inducing effect on insulin fibrillation, whereas B2T_TT showed an inhibitory effect on insulin fibrillation. B2T_TT showed the efficiency to delay the lag phase of insulin fibrillation even after 800 min of incubation at 62 °C. In contrast, B2T_YY and B2T_FF stimulated insulin fibrillation by shortening the lag phase (Fig. 1a). Surprisingly B2T_KV destabilized insulin and promoted its fibrillation to a high extent. Insulin peptide 1 : 1 complex structures were monitored through SEM. After 800 min of incubation, there was no fibrils observed in the insulin−peptide (B2T_TT) complex, while others showed visible morphology like fibrils (Fig. 2a.i–vi).

3.2. Structural transition of insulin and increment of the size of oligomers during fibrillation study by CD and DLS

To attain more gravity in the resolution of insulin−peptide complex we investigated the secondary structural changes of insulin by CD spectroscopy in presence of the peptides. Insulin in presence of B2T_YY, B2T_FF, and B2T_KV showed majorly helices structure at the initial stage (0 min) of the incubation (Fig. 1c). After 80 0 min of heat incubation, we observed that
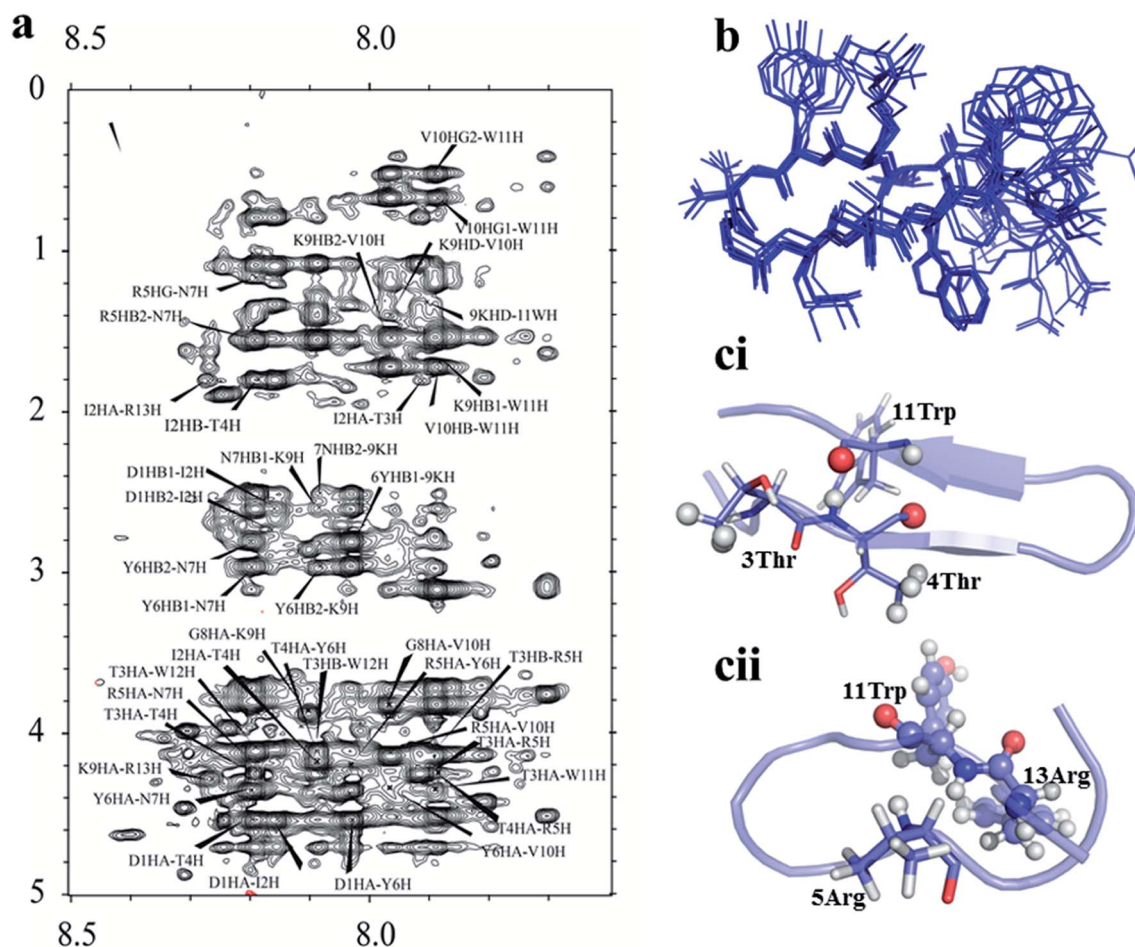
Fig. 4 (a) Noesy spectrum of B2T_TT. (b) Ensemble structure of B2T_TT calculated from CYANA. (c) Comparison of two different types of hairpin structure formed by B2T peptides (ci- B2T_TT and cii-B2T_KV), the orientation actually making B2T_TT a potent inhibitor of insulin fibrillation.

insulin co-incubated with B2T_YY, B2T_FF, and B2T_KV showed a loss of helices and an increment of random coils and β-sheet structures while B2T_TT maintains the native insulin structure (Fig. 1d). The percentage of helices, beta-sheets, and random coils are listed in ESI Table 1(i)–(iv)† DLS data also showed a size increment of insulin in the presence of B2T_YY, B2T_FF, and B2T_KV while no changes in the presence of B2T_TT (Fig. 3a.i–iv) were observed.

3.3. Study of interaction between insulin and hairpin-peptides by ITC and SEC

For a better understanding of inhibition of insulin fibrillation, we performed ITC and size-exclusion chromatography to find out the interaction between insulin and hairpin peptides (Fig. 2b.i–iv and ESI Fig. 5†). We get a sequential binding nature of B2T_TT with insulin monomers with $K_{a1} = 2.3 \times 10^4$ M^{-1}, $K_{a2} = 6.01 \times 10^4$, $K_{a3} = 4.16 \times 10^4$ and $K_{a4} = 2.16 \times 10^4$ M^{-1} (Fig. 3b.iii) indicates (1 : 4) insulin-B2T_TT complex may require for the inhibition. Our previous experiment suggested that insulin: B2T_TT ratio is sufficient to inhibit the fibrillation process of insulin. Insulin: B2T_YY, insulin: B2T_FF and insulin: B2T_KV showed a lower dissociation constant (Fig. 3b.i, b.ii and b.iv) compared to that of insulin: B2T_TT complex. All

other thermodynamic parameters are listed in ESI Table 2a–d.† SEC data suggested that B2T_TT inhibits the fibrillation process of insulin in 1 : 1 complexation, as insulin: B2T_TT complex elutes latter. As the fibrillation occurs and the size of the complexes increases all other peptide insulin complexes (insulin: B2T_YY, insulin: B2T_FF and insulin: B2T_KV) elute at the beginning of the chromatographic run in SEC (ESI Fig. 5†).

3.4. Structural adaptation of all four peptides by TOCSY-NOESY NMR spectroscopy

The four hairpin structure has a common C-terminal nona-meric sequence RYNGKVWWR. The First 4 residues were modified in the 13-meric peptide. B2T_YY contains DMYY, B2T_TT contains DITT, B2T_FF contains DIFF and B2T_KV contains KVYY. B2T_TT differs from B2T_YY by three residues (ITT), B2T_FF by two residues (FF) and B2T_KV by four residues (DITT). We have observed two different types of beta-hairpin structures that were adopted by the four peptides (Fig. 4 and ESI Fig. 1–3†). B2T_TT and B2T_YY adopt a specific hairpin structure with identical fold type where the carboxyl group of 11Trp has interacted with amide group of 4Thr and 4Tyr respectively. This structural orientation influences the side chain of the arginine residues in the 5th position to reside in
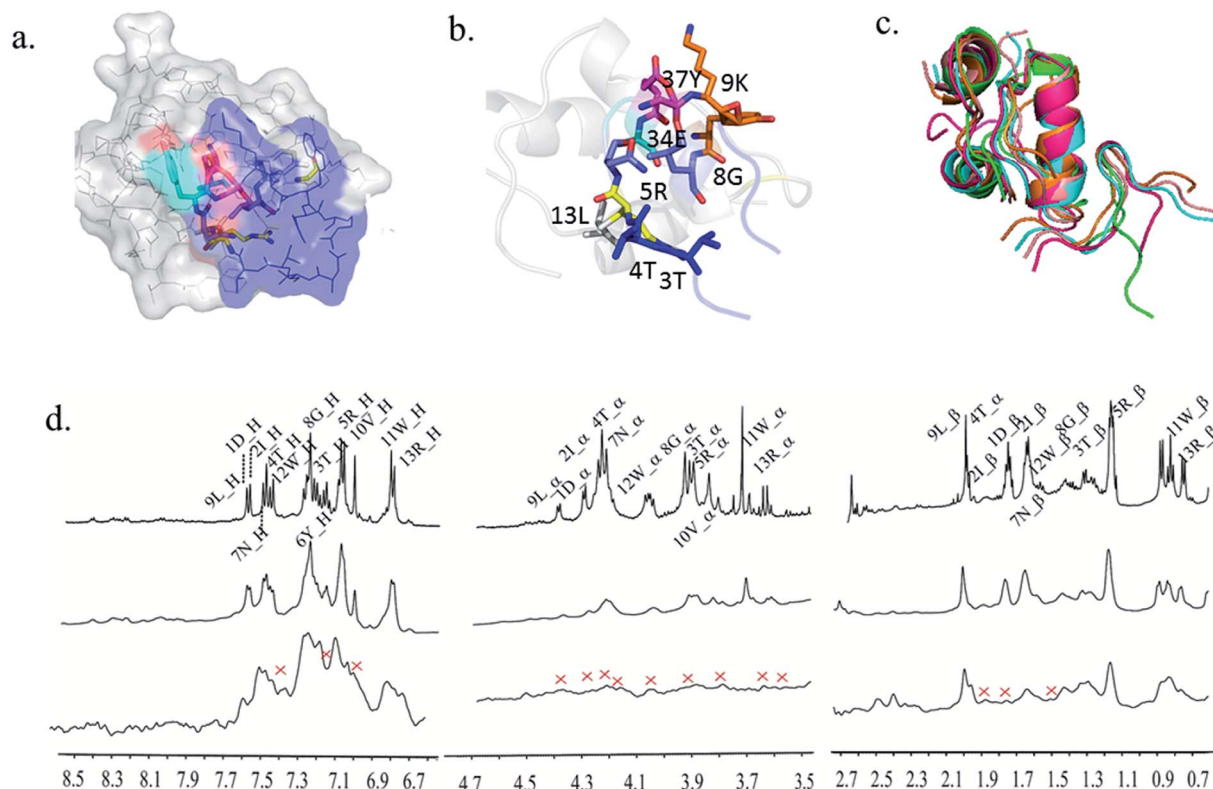
Fig. 5 (a) B2T_TT interacting with insulin's B-chain. (b) The residues of B2T_TT involved in the interaction, (c) 0 ns, 10 ns, 40 ns, 70 ns and 100 ns md simulation run structures of insulin−B2T_TT complex showing peptide binding throughout the 100 ns of md simulation. (d) STD NMR of B2T_TT.

such a position that it can bind with insulin A-chain residue 13Leu. Quite the reverse, B2T_FF and B2T_KV show similar hairpin structures just the opposite conformation than the previous type. In both B2T_FF and B2T_KV, the position of 11Trp is quite different than the B2T_TT and B2T_YY. The carboxyl group of 11Trp is faced towards the outer surface protruding out causing no significant hydrogen bonding between the amide group of 4Phe and 4Tyr respectively. Moreover, (H_2O) OH−π the interaction between 3Phe/4Phe/3Tyr/4Tyr and surrounding H_2O molecules (ESI Fig. 1b & c; 2b & c; 3b & c†) is the predominant factor in stabilizing the beta-hairpin conformation causing 3Phe and 4Tyr residues more dynamic in the water medium, which was missing in case of B2T_TT peptide where 3T and 4T residues repel water molecules keeping the peptide less dynamics and restricting arginine residues on 5th position to arrest the A-chain of insulin. For the former two, B2T_FF and B2T_KV due water-induced dynamicity of 3Y/F, 4Y/F capturing the B chain of insulin by these peptides are in vain.

3.5. The mechanism behind insulin–peptides interaction study by STD-NMR spectroscopy and molecular dynamics simulation

From a mechanistic perspective, it has been observed that the binding of B2T_TT with an insulin monomer prevents the insulin fibrillation process. From previous reports, it is confirmed that during insulin fibrillation the C-terminal of B-

chain (residue 45–50) opens up so that all the hydrophobic residues become exposed and the residues can bind to other residues to forms aggregates.[20,33] Under this consideration, the opening of the C-terminal of B-chain has to be prevented for further dimerization or oligomerization. To study the details mechanism of peptide–insulin interaction we performed STD-NMR (Saturation Transfer Difference) NMR spectroscopy and molecular dynamics (Fig. 5a–d, 3b–c and ESI Fig. 1–3†). Molecular dynamics suggest that 5Arg, 6Tyr, 7Asn, and 8Gly of B2T_TT forms hydrophobic interactions and van der Waals interaction between 41Gly, 38Leu, 35Ala, 34Glu respectively of B-chain of insulin. The 5Arg of B2T_TT interacts with 13Leu A-chain of insulin. This is the crucial binding where 5Arg residues playing the major role of stabilizing insulin monomer. All these possible bindings suggest that B2T_TT stabilizes the opening of the C-terminal of B-chain as well as occupying all the epitopes for fibrils of insulin monomer (30-SHLVEA-35)[20] that were responsible for dimerization. B2T_TT binds with the C-terminal of the B-chain so that insulin remains in the same conformation without exposing its hydrophobic core. 12Trp and 11Trp of B2T_TT bind with B41 and B40 respectively which belong to the helix of B-chain. This helix has the tendency of losing its helicity and forming β-sheet[34,24]. Thus, B2T_TT binds with insulin monomers in a clump like structure. This clump structure blocked the residues majorly involved in the insulin fibrillation process, by stabilizing the flexibility nature of those residues. From STD-NMR also it is confirmed that 4Thr, 11Trp, 5Arg,
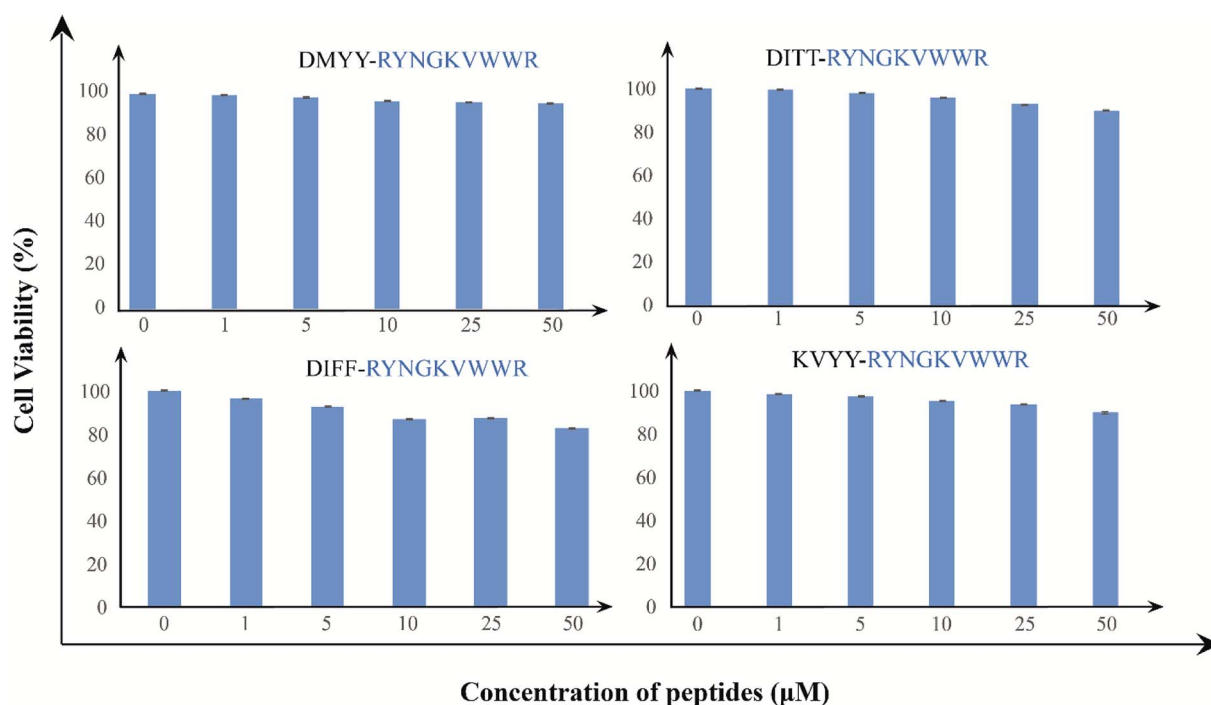
Fig. 6 (a) XTT assay data of B2T_YY, (b) XTT assay data of B2T_TT and (c) XTT assay data of B2T_FF and (d) XTT assay data of B2T_KV. 1 = Controls, 2 = 1 μM, 3 = 5 μM, 4 = 10 μM, 5 = 25 μM and 6 = 50 μM concentration of each peptides.

8Gly, 6Tyr, 13Arg and 9Lys of the peptide bind to insulin monomer (Fig. 5d). The two Thr residues form a 'S' shaped conformation within the hairpin structure making the Arg5 more stable and anchors to staple the A-chain of insulin so that the bindings between RYNG of B2T_TT with a helix of B-chain of insulin remains stable. Also, a very strong hydrogen bonding was found between 8Gly and 9Lys of B2T_TT with 37Tyr and 38Leu respectively. We found all these interactions all along the 100 ns of simulation run (Fig. 5c). All the total 100 ns of MD simulation of insulin and insulin–peptides complexes are shown in ESI Fig. 7a–e.†

We have run 100 ns MD simulation of insulin and insulin–peptide complexes. We have calculated the RMSD value and RMSF value from the total run. The RMSD value implies the stability of insulin and insulin–peptide complex and RMSF value implies the total fluctuation of residues of insulin. Insulin shows an increasing RMSD value for 60 ns. The RMSD value rises up to 8.5 Å. After 60 ns the RMSD value fluctuates and gradually decreases to 4 Å. Insulin–B2T_TT complex shows a low RMSD value for 45 ns and then rises to 4 Å and was stable for 100 ns indicating B2T_TT upon binding stabilizes insulin (ESI Fig. 4a†). Insulin–B2T_YY complex, insulin–B2T_FF complex and insulin–B2T_KV complex shows high RMSD value which indicates these peptides are not efficient to stabilize insulin. The RMSF value was also shown in ESI Fig. 4b.†

3.6. Cell toxicity assay of all four peptides by XTT-assay

Finally, we examine the cytotoxic effects of the peptides; we have treated HEK293 cell lines with B2T_YY, B2T_TT, B2T_FF, and B2T_KV with increasing concentration gradient (0–50 μM) for 24 hours, and monitored cell proliferation by XTT assay. There has been no marked reduction in cell proliferation after 24 hours of treatment. All these four peptides induce meager to no cytotoxicity to HEK293 cells even at 50 μM (cell viability-95.6%, 89.9%, 82.5%, and 89.5% respectively) concentration (Fig. 6). These non-toxic natures of the peptides establish them as a safe and tolerant drug for normal tissue use.

4. Conclusion

In conclusion, from thioflavin T assay, CD spectroscopy and DLS we can say that insulin upon binding with B2T_TT delays insulin fibrillation process even after 800 min of heat incubation. SEM images suggest that there are no such morphological changes in the presence of B2T_TT in the insulin–peptide complex (insulin: B2T_TT). Here in this study, we designed such a beta-hairpin structure that binds with insulin monomers and prevents its fibrillation process. Our study has two significant prospects: (a) In future this type of peptide will open the path for treating different types of diseases caused by protein aggregation and (b) this type of peptide can be used as an insulin stabilizer. Therefore, we can suggest that beta-hairpin peptide can be used as a therapeutic drug in the future.

Conflicts of interest

There are no conflicts to declare.

Acknowledgements

References

1 C. M. Dobson, *Nature*, 2003, **426**, 884–890.

2 J. D. Sipe and A. S. Cohen, *J. Struct. Biol.*, 2000, **130**, 88–98.

3 E. Kachooei, A. A. Moosavi-Movahedi, F. Khodagholi, H. Ramshini, F. Shaerzadeh and N. Sheibani, *PLoS One*, 2012, **7**, e41344.

4 F. Chiti, P. Webster, N. Taddei, A. Clark, M. Stefani, G. Ramponi and C. M. Dobson, *Proc. Natl. Acad. Sci. U.S.A.*, 1999, **96**, 3590–3594.

5 C.-C. Lee, A. Nayak, A. Sethuraman, G. Belfort and G. J. McRae, *Biophys. J.*, 2007, **92**, 3448–3458.

6 J. L. Jimenez, E. J. Nettleton, M. Bouchard, C. V. Robinson, C. M. Dobson and H. R. Saibil, *Proc. Natl. Acad. Sci. U.S.A.*, 2002, **99**, 9196–9201.

7 G. Biolo, B. D. Williams, R. Fleming and R. R. Wolfe, *Diabetes*, 1999, **48**, 949–957.

8 A. Basu, C. Dalla Man, R. Basu, G. Toffolo, C. Cobelli and R. A. Rizza, *Diabetes Care*, 2009, **32**, 866–872.

9 Q.-x. Hua and M. A. Weiss, *J. Biol. Chem.*, 2004, **279**, 21449–21460.

10 N.-T. Yu and C. Liu, *J. Am. Chem. Soc.*, 1972, **94**, 3250–3251.

11 N.-T. Yu, C. Liu and D. O'shea, *J. Mol. Biol.*, 1972, **70**, 117–132.

12 P. Westermark and E. Wilander, *Diabetologia*, 1983, **24**, 342–346.

13 D. M. Walsh, I. Klyubin, J. V. Fadeeva, W. K. Cullen, R. Anwyl, M. S. Wolfe, M. J. Rowan and D. J. Selkoe, *Nature*, 2002, **416**, 535–539.

14 K. Huang, J. Dong, N. B. Phillips, P. R. Carey and M. A. Weiss, *J. Biol. Chem.*, 2005, **280**, 42345–42355.

15 J. Sharp, J. Forrest and R. Jones, *Biochemistry*, 2002, **41**, 15810–15819.

16 D. F. Waugh, *J. Am. Chem. Soc.*, 1946, **68**, 247–250.

17 M. J. Burke and M. A. Rougvie, *Biochemistry*, 1972, **11**, 2435–2439.

18 G. Glenner, E. Eanes, H. Bladen, R. Linke and J. Termine, *J. Histochem. Cytochem.*, 1974, **22**, 1141–1158.

19 J. Brange, L. Andersen, E. D. Laursen, G. Meyn and E. Rasmussen, *J. Pharm. Sci.*, 1997, **86**, 517–525.

20 H. H. Lee, T. S. Choi, S. J. C. Lee, J. W. Lee, J. Park, Y. H. Ko, W. J. Kim, K. Kim and H. I. Kim, *Angew. Chem., Int. Ed.*, 2014, **53**, 7461–7465.

21 V. Banerjee, R. K. Kar, A. Datta, K. Parthasarathi, S. Chatterjee, K. P. Das and A. Bhunia, *PLoS One*, 2013, **8**, e72318.

22 M. Zaman, M. V. Khan, S. M. Zakariya, S. Nusrat, S. M. Meeran, P. Alam, M. R. Ajmal, W. Wahiduzzaman, Y. E. Shahein and A. M. Abouelella, *J. Cell. Biochem.*, 2018, **119**, 3945–3956.

23 T. Saithong, T. Thilavech and S. Adisakwattana, *Int. J. Biol. Macromol.*, 2018, **113**, 259–268.

24 Q. Hua and M. A. Weiss, *Biochemistry*, 1991, **30**, 5505–5515.

25 R. Khurana, C. Ionescu-Zanetti, M. Pope, J. Li, L. Nielson, M. Ramírez-Alvarado, L. Regan, A. L. Fink and S. A. Carter, *Biophys. J.*, 2003, **85**, 1135–1144.

26 M. I. Ivanova, S. A. Sievers, M. R. Sawaya, J. S. Wall and D. Eisenberg, *Proc. Natl. Acad. Sci. U.S.A.*, 2009, **106**, 18990–18995.

27 D. Rajamani, S. Thiel, S. Vajda and C. J. Camacho, *Proc. Natl. Acad. Sci. U.S.A.*, 2004, **101**, 11287–11292.

28 W. Wang and M. H. Hecht, *Proc. Natl. Acad. Sci. U.S.A.*, 2002, **99**, 2760–2765.

29 W. Hosia, N. Bark, E. Liepinsh, A. Tjernberg, B. Persson, D. Hallén, J. Thyberg, J. Johansson and L. Tjernberg, *Biochemistry*, 2004, **43**, 4655–4661.

30 B. G. Pierce, K. Wiehe, H. Hwang, B. H. Kim, T. Vreven and Z. Weng, *Bioinformatics*, 2014, **30**(12), 1771–1773.

31 J. Wang, R. M. Wolf, J. W. Caldwell, P. A. Kollman and D. A. Case, *J. Comput. Chem.*, 2004, **25**(9), 1157–1174.

32 J. A. Maier, C. Martinez, K. Kasavajhala, L. Wickstrom, K. E. Hauser and C. Simmerling, *J. Chem. Theory Comput.*, 2015, **11**, 3696–3713.

33 L. Nielsen, R. Khurana, A. Coats, S. Frokjaer, J. Brange, S. Vyas, V. N. Uversky and A. L. Fink, *Biochemistry*, 2001, **40**, 6036–6046.

34 R. L. Millican and D. N. Brems, *Biochemistry*, 1994, **33**, 1116–1124.